

Modeling and Spatialization of Biomass and Carbon Stock Using Lidar Metrics in Tropical Dry Forest, Brazil: Preliminary Results

Robson Borges de Lima (✉ rbl_florestal@yahoo.com.br)

Universidade do Estado do Amapá <https://orcid.org/0000-0001-5915-4045>

Cinthia Pereira de Oliveira

Universidade do Estado do Amapá

Rinaldo Luiz Caraciolo Ferreira

Universidade Federal Rural de Pernambuco

José Antônio Aleixo da Silva

Universidade Federal Rural de Pernambuco

Emanuel Araújo Silva

Universidade Federal Rural de Pernambuco

Anderson Francisco da Silva

Universidade Federal Rural de Pernambuco

Josias Divino Silva de Lucena

Universidade Federal Rural de Pernambuco

Nattan Adler Tavares dos Santos

Universidade Federal Rural de Pernambuco

Iran Jorge Corrêa Lopes

Universidade Federal do Paraná

Mayara Maria de Lima Pessoa

Universidade Federal Rural de Pernambuco

Cybelle Laís Souto-Maior Sales de Melo

Universidade Federal Rural de Pernambuco

Research

Keywords: Caatinga domain, Forest management, Allometry, Statistical models

Posted Date: August 11th, 2020

DOI: <https://doi.org/10.21203/rs.3.rs-55277/v1>

License:  This work is licensed under a Creative Commons Attribution 4.0 International License.

[Read Full License](#)

1 **Modeling and Spatialization of Biomass and Carbon Stock Using Lidar Metrics**
2 **in Tropical Dry Forest, Brazil: Preliminary Results**

3
4 Cinthia Pereira de Oliveira¹, Rinaldo Luiz Caraciolo Ferreira² José Antônio Aleixo da
5 Silva² Robson Borges de Lima^{1*}, Emanuel Araújo Silva², Anderson Francisco da
6 Silva², Josias Divino Silva de Lucena², Nattan Adler Tavares dos Santos², Iran Jorge
7 Corrêa Lopes³, Mayara Maria de Lima Pessoa², Cybelle Laís Souto-Maior Sales de
8 Melo²

9
10 * Corresponding author: Robson Borges de Lima - rbl_florestal@yahoo.com.br

11
12 ¹ Laboratório de Manejo Florestal, Universidade do Estado do Amapá, Rua Presidente
13 Vargas, nº 450, Centro, Macapá, Amapá, CEP 68901–262, Brasil

14
15 ² Laboratório de Manejo de Florestas Naturais “José Serafim Feitosa Ferraz”,
16 Departamento de Ciência Florestal, Universidade Federal Rural de Pernambuco, Rua
17 Dom Manuel de Medeiros, s/n - Dois Irmãos, Recife, Pernambuco, CEP 52171-900,
18 Brasil

19
20 ³ Departamento de Ciência Florestal, Universidade Federal do Paraná, Av. Prefeito
21 Lothário Meissner, 632 - Jardim Botânico, Curitiba - PR, CEP 80210-170

22 **Email address** cinthia.florestal@gmail.com; rinaldo.ferreira@ufrpe.br;
23 jaaleixo@uol.com.br; rbl_florestal@yahoo.com.br; emanuel.araujo@ufrpe.br;
24 engf.anderson@gmail.com; josiaslucenaeng@gmail.com; nattantavares@gmail.com;
25 iranjorge.@hotmail.com; maypessoa@gmail.com; engf.cybelle@gmail.com

27

28 **Abstract**

29 **Background:** In recent years, with the growing environmental concern regarding
30 climate change, there has been a search for efficient alternatives in indirect methods for
31 studies on the quantification of biomass and forest carbon stock. In this article, we seek
32 to obtain pioneering and preliminary results of estimates of biomass and carbon using
33 data from conventional forest inventory and LiDAR technology in a dry tropical forest
34 in Brazil. We used data from conventional forest inventory in two areas together with
35 data from the LiDAR overflight, generating local biomass estimates from a developed
36 local equation and the carbon levels obtained from local species. With data from LiDAR
37 technology, we extracted the metrics from the point cloud and were used as an
38 independent variable. For the construction of the biomass and carbon allometric models
39 per hectare, we approach three types of models for data analysis: Multiple linear
40 regression with Principal Components - PCA, Conventional multiple linear regression
41 and Multiple linear regression with Stepwise, the generated equations were analyzed by
42 comparisons of statistical criteria (R^2_{aj} and RMSE). After selecting the best equation,
43 we generate the carbon estimates by area by assessing the plot level.

44 **Results:** The best fit TAGB and TAGC model was the multiple linear regression with
45 Stepwise, concluding, then, that LiDAR data can be used to estimate biomass and total
46 carbon in dry tropical forest, proven by an adjustment considered in the models
47 employed, with a significant correlation between the LiDAR metrics.

48 **Conclusions:** Our preliminary results provide important information about the spatial
49 distribution of TAGB and TAGC in the study area, which can be used to manage the
50 reserve for optimal carbon sequestration.

51

52 **Keywords:** Caatinga domain, Forest management, Allometry, Statistical models

53 **Introduction**

54 The increase in the carbon dioxide concentration (CO₂) in the atmosphere in the last
55 decades and its consequences on the environment have been attracting the attention of
56 society and being addressed as a matter of global controversy (Crowther et al. 2015).
57 The high CO₂ concentration in the atmosphere is worrying, as it generates an increase in
58 the greenhouse effect, and consequently causes global warming (Achard and House
59 2015; Coomes et al. 2017; Brahma et al. 2018). In this scenario, dry tropical forest areas
60 play an important role, and the Caatinga vegetation in northeastern Brazil significantly
61 contributes to the global carbon cycle through the aboveground biomass and carbon
62 stock (Sampaio and Silva 2005; Althoff et al. 2018).

63 There is currently a rich ongoing discussion among scientists around the world
64 about the main tools and methods for generating measures to mitigate climate change.
65 The first guiding question to be answered is “how do we measure the impacts of global
66 climate change and how can we slow its progress?” The second key question is “what
67 tools and methods should be used to ensure a reliable estimate?” In many cases, the
68 variables best known for generating rapid responses for dry tropical forest ecosystems
69 are aboveground biomass and carbon.

70 However, the destructive sampling of trees is a limiting factor for calibrating
71 statistical models, mainly due to the high cost employed in field work (Duncanson et al.
72 2017). These methods are currently based on forest inventory data using carbon factors
73 and equations which transform the biometric parameters of the forest such as diameter
74 at breast height (DBH) and height (Ht) of individuals in estimating the carbon stock
75 contained in aboveground forest biomass (Somogyi et al. 2007).

76 Remote sensing techniques combined with optical sensors have recently been
77 presented as a viable alternative for estimating the biomass and carbon stock in planted
78 and natural forests (Silva et al. 2016; Silva et al. 2017a). Among the current remote
79 sensing techniques, laser tillering, also known as LiDAR (Light Detection and Raging),
80 has prominently emerged in the forest scenario (Li et al. 2017), by which biomass and
81 carbon stock estimates can be systematically and efficiently obtained in the field
82 (Duncanson et al. 2017).

83 LiDAR is an active system, and its principle consists of emitting a laser pulse
84 which interacts with an object on the earth's surface and subsequently returns to the
85 sensor in a given time interval. The technology makes it possible to accurately
86 reproduce Digital Terrain Models (DTM, models which enable describing the elevation
87 of land free of objects), Digital Surface Models (DSM, models which enable describing
88 the elevation of the terrain including the objects present), and Digital Height Models
89 (DHM, models which describe the height of all objects, with the cloud points referring
90 to the ground normalized to zero).

91 Although LiDAR technology is an efficient alternative and widely applied in
92 forest inventory in countries like the United States, Finland and Sweden, there are still
93 obstacles to its use in other countries such as Brazil. The limitations are not due to the
94 functioning of the technology itself, but mainly because it is still an emerging
95 technology in Brazil (Silva et al. 2017b). The elaboration of processing methodologies
96 aimed at Brazilian needs is still recent, and in this respect the execution of this work is
97 mainly justified by the search for a scientific technical advance which provides
98 developing routines which can assist in LiDAR data acquisition and processing, and in
99 turn seeking to efficiently attain above-ground biomass and carbon stock estimates in a
100 Brazilian dry tropical forest.

101 In particular, LiDAR technology has the ability to directly measure the
102 vegetation attributes (metrics) on a vertical scale with high precision, and therefore a
103 system can be developed to sample the biomass and carbon stock of the trees in situ in
104 environmental gradients, providing a potential solution to outstanding problems related
105 to forest biomass and above-ground carbon stock (Saatchi et al. 2009; Avitabile et al.
106 2011). Biomass and carbon estimates at local and regional levels, as well as the
107 spatialization of these variables using maps can provide an overview of biodiversity and
108 forest structure (Martinuzzi et al. 2013; Nelson et al. 2017; Becknell et al. 2018). This
109 information is extremely important for the caatinga vegetation domain in Pernambuco
110 for possible payments for environmental services and other projects aimed at reducing
111 emissions from deforestation and forest degradation (REDD +).

112 Due to the great importance of caatinga forest resources, quantifying and
113 mapping biomass and carbon stock using LiDAR metrics is a key factor to meet the
114 legal aspects concerning sustainable management, mainly reconciling sustainable wood
115 production and stock maintenance of carbon in the area. This task is one of the main
116 long-term planning tools, because in addition to dimensioning the forest's stock and
117 productivity, it generates information which will direct ecosystem maintenance through
118 conservation and/or preservation (Mohebalian and Aguilar 2018).

119 In this sense, this work was developed with the intention of generating
120 information on biomass and carbon stock using LiDAR metrics in different dry tropical
121 forest areas in the municipality of Floresta, Pernambuco. Specifically, it is intended to:
122 a) Estimate the total biomass and carbon stock for the parcels inventoried in two areas
123 using a local allometric model; b) Use the aerial LiDAR system to generate attributes in
124 plots in the different dry forest areas inventoried in Pernambuco; c) Develop an
125 allometric model for estimating biomass and carbon stock using LiDAR metrics for the

126 different dry forest areas inventoried in Pernambuco; d) Generate biomass and carbon
127 stock maps for the different dry forest areas inventoried in Pernambuco.

128 **Results**

129 ***Preliminary results***

130 The average minimum and maximum elevation values which correspond to the tree
131 heights obtained by the LiDAR metrics ranged from 1.49 to 4.77 meters with an
132 average of 3.06 m for the *Correntão* area. There is little difference in the minimum
133 elevations per plot (1.39 m) for the *Transposição* area, but this area had the lowest
134 average elevation (2.88 m) and the highest maximum elevation (5.05 m). The highest
135 biomass and total carbon concentration per hectare was observed in the *Correntão* area
136 with values ranging from 0.61 to 129 Mg.ha⁻¹, with an average of 24.93. TAGB
137 estimates for all plots in the *Transposição* area ranged from 1.22 to 29.37 Mg.ha⁻¹, with
138 an average value of 9.32 Mg.ha⁻¹.

139 The component loads (correlations between each variable and each principal
140 component), the eigenvalues and the variation percentage of the principal components
141 for the LiDAR metrics for the *Transposição* and *Correntão* areas are shown in Tables 4
142 and 5, respectively. The principal component analysis of the *Transposição* metrics
143 produced three principal components which synthesized 85.6% of the variability in the
144 data. The first principal component (PC1) of the metrics in this area had a high load of
145 all variables with maximum contribution from the average increase (0.996). The
146 principal component analysis for the metrics of the *Correntão* area also produced three
147 principal components which synthesized 82.8% of the variability in the data. The first
148 principal component (PC1) for the metrics in this area had maximum loads for
149 maximum elevation and average elevation. The principal components which only
150 represented a small amount of variance were not used in the regression analysis.

151

152 Table 4. Component loads, eigenvalues and percentage of variation of the main
153 components (PC) for the LiDAR metrics in the Transposição area.

Principal component	Components (eigenvectors)											
	Elev. minimum	Elev. maximum	Elev. mean	Elev. mode	Elev. stddev	Elev. CV	Elev. skewness	Elev. kurtosis	Elev. MAD. median	Elev. P01	Auto valores	Var (%)
PC1	0.285	0.678	0.996	0.759	0.719	0.333	-0.231	-0.192	0.689	0.420	12.463	51.929
PC2	-0.395	0.621	0.070	-0.020	0.675	0.902	0.738	0.151	0.590	-0.508	5.841	76.266
PC3	0.622	0.281	-0.009	-0.070	-0.027	0.016	0.597	0.672	-0.203	0.602	2.255	85.663

154

155 Table 5. Component loads, eigenvalues and percentage of variation of the main
156 components (PC) for the LiDAR metrics in the *Correntão* area.

Principal component	Components (eigenvectors)											
	Elev. minimum	Elev. maximum	Elev. mean	Elev. mode	Elev. stddev	Elev. CV	Elev. skewness	Elev. kurtosis	Elev. MAD. median	Elev. P01	Auto valores	Var(%)
PC1	0.019	0.825	0.999	0.709	0.708	0.158	-0.192	0.170	0.557	0.305	13.233	55.136
PC2	-0.130	0.423	0.018	-0.302	0.675	0.943	0.708	-0.179	0.633	-0.234	4.119	72.299
PC3	0.765	-0.283	0.016	-0.106	0.074	0.110	-0.103	-0.805	0.359	0.636	2.524	82.815

157

158 The results of the step-by-step regression analysis for each area are shown in
159 Table 6. The variables which did not significantly contribute to the TAGB prediction
160 for each area were simultaneously eliminated during the analysis. The determination
161 coefficient (R^2_{aj}) of the models for the *Transposição* area varied from 0.17 to 0.42 and
162 the RMSE varied from 3.18 to 5.99 Mg.ha⁻¹. Models with higher R^2 values and lower
163 RMSE indicate better TAGB prediction. Models developed using the principal
164 component technique of the LiDAR metrics for each area generally had an
165 unsatisfactory performance.

166

167 Table 6. Multiple linear regression models adjusted for the biomass estimate, obtained
168 by LiDAR data

169

170

171

Area	Biomass predictive models	R ² ajd	RMSE
<i>Transposição</i>	TAGB = - 86.809 -33.295(Elev.minimum) + 5.446(Elev.maximum) + 195.226(Elev.mean) + 3.774 (Elev.mode) -92.658(Elev.stddev) + 206.851(Elev.CV) + 13.627(Elev.skewness) -1.734 (Elev.kurtosis) + 24.360(Elev.MAD.median) + 29.676(Elev.P01) - 25.707(Elev.P10) -64.704(Elev.P20) + 49.118(Elev.P25) -26.958(Elev.P30) -44.133(Elev.P50) -21.226(Elev.P60) -11.419(Elev.P75) 2.295(Elev.P80) - 27.855(Elev.P90) -15.740(Elev.P95) + 98.142(Canopy.relief.ratio) + 0.024(Percentage.all.returns.above.1.30)	0.1924	3.18
	TAGB = -21.08 -35.756(Elev.minimum) + 119.784 (Elev.mean) + 4.582(Elev.mode) -63.752 (Elev.stddev) + 101.103(Elev.CV) + 27.823(Elev.P01) -17.626(Elev.P10) -29.152(Elev.P20) - 44.745(Elev.P50) -18.032(Elev.P90)	0.4239	3.51
	PCA regression TAGB = 9.145 + 0.607(Dim.1) + 1 (Dim.3)	0.1723	5.99
<i>Correntão</i>	TAGB = 341.760 + 0.932(Elev.minimum) + 123.520(Elev.maximum) -298.028(Elev.mean) + 1.734(Elev.mode) -14.288(Elev.stddev) + 712.426(Elev.CV) -8.027(Elev.skewness)- 36.267(Elev.kurtosis) + 103.257(Elev.MAD.median) +114.736(Elev.P01) + 79.665(Elev.P10) + 54.843(Elev.P20) + 39.873(Elev.P25) + 90.032(Elev.P30) + 20.564(Elev.P50) + 5.063(Elev.P60) -129.573(Elev.P75) -33.779(Elev.P80) + 57.286(Elev.P90) 53.403(Elev.P95) + 519.378(Canopy.relief.ratio) - 0.103(Percentage.all.returns.above.1.30)	0.4239	13.61
	TAGB = -269.86 + 145.44(Elev. maximum) - 402.19(Elev.mean) + 440.13(Elev.CV) - 53.26(Elev.kurtosis) + 88.49(Elev.P01) + 93.09(Elev.P10) + 165.73 (Elev.P30) -67.6(Elev.P75) + 673.35(Canopy.relief.ratio)	0.533	14.76
	PCA regression TAGB = 30.270-6.465 (Dim.3)	0.09621	28.45

172

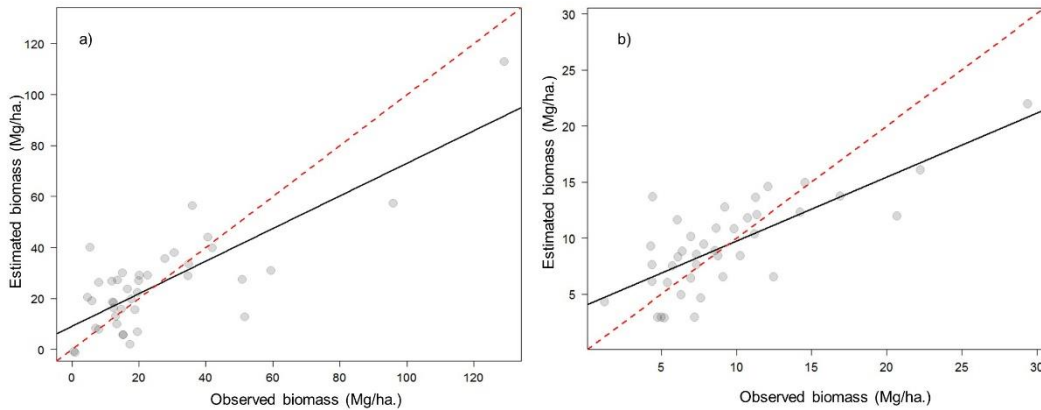
173

174

175

The models which combined the step-by-step selection of the metrics showed better results in both areas compared to models which use the traditional multiple

176 regression modeling, although the prediction error of the multiple model was slightly
177 lower. Based on the adjustment statistics, the Stepwise regression model was considered
178 the most suitable for predicting TAGB for both areas and this can be illustrated in the
179 figure 5.

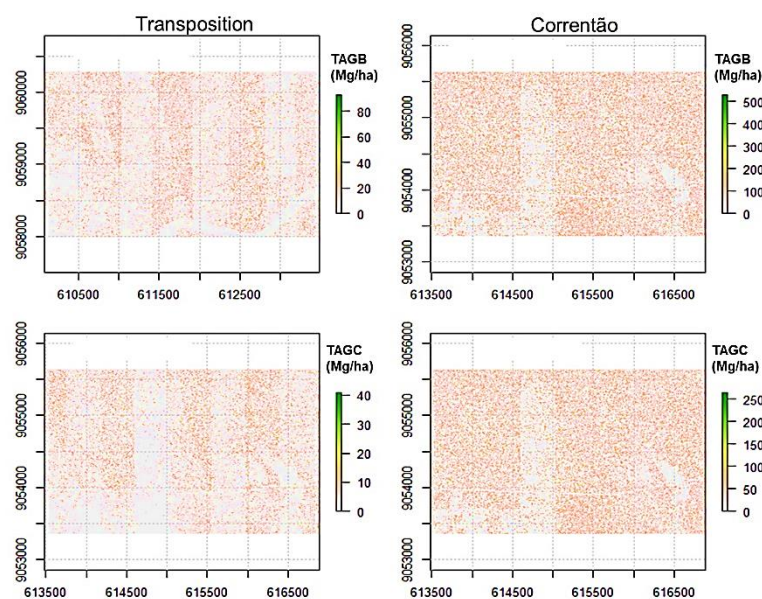


180
181 **Fig. 5** Predictions of the best allometric equations for the *Correntão* area (a) and
182 *Transposição* (b) using the LiDAR metrics selected step by step in relation to the
183 observed values. The solid black line indicates the fit of the equation and the red dotted
184 line indicates the ideal fit in a 1: 1 ratio.

185
186 The most significant predictor variables for the model for the *Transposição* area,
187 and therefore the most suitable for predicting local TAGB, were Elev.minimum,
188 Elev.maximum, Elev.mean and Elev.P01; the last two were found in all tested models.
189 The final model for the *Correntão* area predicts that the total biomass stock may be
190 more significant from the Elev metrics. Maximum, Elev.mean, Elev.CV, Elev.kurtosis,
191 Elev.P01, Elev.P10, Elev.P30, Elev.P75 and Canopy.relief.ratio.

192 The Stepwise regression model was applied to map the density of TAGB in the
193 study areas (Fig. 6). The TAGB map was converted to carbon stock/Mg.ha⁻¹ (TAGC)
194 maps to predict the total stock in the areas using the average carbon fraction (0.48), as
195 estimated in this study. The estimated average density of TAGB and TAGC for the

196 *Transposição* area was $9.2 \pm 6.1 \text{ Mg}\cdot\text{ha}^{-1}$ and $4.6 \pm 14 \text{ Mg}\cdot\text{ha}^{-1}$, respectively. Most plots
197 in both areas had a low density of TAGB above $30 \text{ Mg}\cdot\text{ha}^{-1}$ (85.8%), storing
198 approximately 44.1% of the TAGC stock. About 1.2% of the forest stand in the area in
199 both locations had a TAGB density greater than $50 \text{ Mg}\cdot\text{ha}^{-1}$. Areas with TAGB below
200 $100 \text{ Mg}\cdot\text{ha}^{-1}$ cover about 99% of the forest stand. Low density areas of TAGB and
201 TAGC, as shown in the maps, are potential areas for assisted regeneration and
202 enrichment planting to increase the carbon sequestration capacity of the forest stand.



203
204 **Fig. 6** Spatialization of biomass and carbon based on Stepwise regression models
205 defined according to the LiDAR metrics for the *Transposição* and *Correntão* areas.

206
207 When comparing the areas, it is noted that the most preserved area
208 (*Transposição*) presented a lower carbon stock than the most degraded area (*Correntão*)
209 (Fig. 6). This can be explained in the inventories carried out in the degraded area, which
210 showed individuals with greater dominance than in the preserved area, strongly
211 influencing the predicted biomass and carbon values.

212 These results are not only absolute numbers of the inventoried variables, but also
213 other variables obtained from the LiDAR technology and should be considered for

214 better interpretation of the results obtained in this work, namely: the density of pulses
215 emitted by LiDAR, the characteristics of the vegetation trunks/stems studied and the
216 effect of water stress on leaves.

217

218 **Discussion**

219 The preliminary results of this study indicate that the LiDAR metrics provided reliable
220 estimates of TAGB and TAGC for the two study areas. The results show a good
221 statistical relationship between field biomass data and height (elevation) metrics,
222 suggesting that it is an important predictor of local biomass, especially when selected
223 using the Stepwise method. However, the relationship was weaker in both areas when
224 all metrics were incorporated into the traditional modeling process or when using
225 regression with principal components. Only the individual categories of the height
226 metrics (minimum, average and maximum) explained more than 40% of the variance.
227 This suggests that the incorporation of height data may be necessary to improve the
228 prediction of TAGB and TAGC.

229 The R^2 and RMSE values of the best-fit models vary in similar studies which
230 used LiDAR data and metrics to estimate and map the aboveground biomass of trees in
231 dry forests. (Anderson et al. 2018) reported R^2 values ranging from 0.36 to 0.71 and
232 RMSE values from 99 to 175 $\text{Mg}\cdot\text{ha}^{-1}$ in Idaho (USA) based on machine learning data.
233 In a dry tropical forest in Mexico, (Hernández-Stefanoni et al. 2015) reported R^2 from
234 0.77 and RMSE from 21.6 to 25.7 $\text{Mg}\cdot\text{ha}^{-1}$ based on linear regression and LiDAR data.
235 Also in Idaho (USA), (Li et al. 2017) reported R^2 of 0.87 and RMSE of 3.59 kg based
236 on linear regression and data on percentage plant cover derived from ALS. (Chen et al.
237 2015) reported R^2 ranging from 0.38 to 0.64 in the Amazon based on mixed-effect

238 models and LiDAR data from agroforestry systems. The biomass estimates by the tested
239 methodologies showed satisfactory and promising results in all of these cases.

240 The best-fit TAGB model consisted of 10 LiDAR predictor variables for the
241 *Transposição* area and 9 LiDAR predictor variables for the *Correntão* area. These
242 variables indicate that the vertical profile of vegetation at different elevations
243 (minimum, medium and maximum heights) are potential predictors for TAGB. TAGB
244 estimation and mapping for the studied forest was based on the best-fit model.

245 The spatial distribution pattern of TAGB is related to the structure and
246 composition of the forest landscape, where low TAGB areas correspond to low forest
247 cover areas, while high biomass areas correspond to densely forested areas. The overall
248 average TAGB of 32 Mg.ha⁻¹ for two areas is comparable and is within the range of
249 values reported for mature dry tropical forests in previous studies, indicating that the
250 modeling approach used in this study provides reasonable predictions of TAGB
251 (Martinuzzi et al. 2013; Kachamba et al. 2017; Naveenkumar et al. 2017).

252 Uncertainties in the TAGB estimates in this study could result from errors
253 associated with field measurements, however plot TAGB estimates are based on a
254 location-specific allometric equation with the breadth of data covering a wide sample in
255 the model development, showing an accurate TAGB estimate. Any errors associated
256 with the TAGB estimate at the plot level using a pantropical equation would propagate
257 to the TAGB regression model, and therefore to the TAGB estimates (Chave et al.
258 2005; Chave et al. 2014). However, another possible source of error in biomass
259 predictions may be the density of points adopted, as 0.5 (pulses/m²) were adopted in the
260 data used, while carbon quantification works generally work with 4 to 25 points (Silva
261 et al. 2014; Figueiredo et al. 2016; Nelson et al. 2017; Coomes et al. 2017). Through
262 tests with point density, Silva et al. (2017) found that its reduction can result in a

263 decrease in R^2 and an increase in RMSE, in addition to increasing the variance of AGB
264 estimates. (Leitold et al. 2015) obtained bias in height estimates which translated into
265 errors of 80-125 Mg.ha⁻¹, when the operator worked with the pulse density below 4 m².

266 Pulse densities from moderate to high changes are invariant and only relatively
267 little affect results; however, once the pulse drops to 1/m², it makes metrics related to
268 coverage (canopy coverage, tree density and shrub coverage) more sensitive to changes
269 in this density (Magnusson et al. 2007). Thus, the increase in RMSE can be explained
270 by the less accurate classification of soil returns (Silva et al. 2017a; Silva et al. 2017b).
271 However, it is worth noting that the low density of points can also be related to good
272 results, depending on the variable to be studied, such as canopy metrics (Thomas et al.
273 2006) or volume (Takahashi et al. 2010). In addition, the TAGC for the study area was
274 estimated based on the TAGB and the average carbon fraction of the trees; any errors in
275 the TAGB estimate would extend to the TAGC estimates. However, the results of this
276 study indicate that the TAGB model provided reliable TAGB estimates for the study
277 area.

278

279 **Conclusions**

280 According to the results found in this work, we concluded that LiDAR data can be used
281 for estimating biomass and total carbon in dry tropical forest, as confirmed by an
282 adjustment considered in the models used, with good correlation between the LiDAR
283 metrics and the biomass data observed in the field. More specifically, we have the
284 following conclusions and recommendations for future work:

285

286 i) Using Stepwise to reduce the metrics proved to be more effective for better
287 adjustment of the models;

288

289 ii) The LiDAR metrics which were most present in the models were: Elev.minimum,
290 Elev.maximum, Elev.mean and Elev.P01, with the last two being found in all models;

291

292 iii) The most preserved area had a lower carbon stock than the most degraded area, this
293 occurrence can be explained in the inventories carried out in the area that showed a
294 higher DAB number in the degraded area than in the preserved area, strongly
295 influencing the estimated carbon values in the areas;

296

297 iv) The pulse density, even though it is not a variable within the models, indirectly
298 influenced the accuracy of the models, therefore, it is recommended that data be tested
299 with a higher pulse density in future works.

300

301 v) The model is limited to the TAGB estimate in the study area and may not be suitable
302 for application in other forests. This is due to differences in forest structure, species
303 composition, vegetation vigor and impacts of atmospheric conditions and soil moisture
304 and precipitation.

305

306 vi) New studies are recommended to assess the transferability of the model to other
307 protected forests with forest structure and similar species composition. Other studies
308 that will test the ability of non-parametric algorithms (such as random forest) to develop
309 TAGB estimation models for the study area, in comparison with linear regression
310 analysis, are also recommended.

311

312 vii) Our preliminary results provided important information on the spatial distribution of
313 TAGB and TAGC in the study area, which can be used to manage the reserve for
314 optimal carbon sequestration.

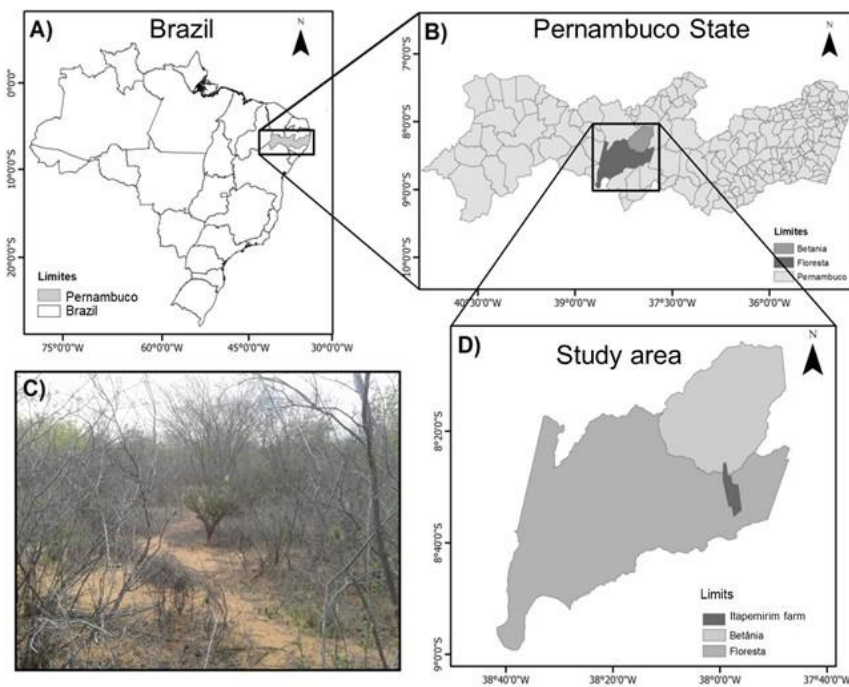
315

316 **Materials and methods**

317 **Study area**

318 The work was carried out in two semiarid areas of Itapemirim farm. Its extension is
319 approximately 60 km² (Fig. 1 D), located in the Municipality of Floresta in the São
320 Francisco mesoregion in Pernambuco, northeast Brazilian (8° 30' 37" S and 37° 59' 07"
321 W).

322



323

324 **Fig. 1** Coverage of the study area: A, B and D, and profile photo in Floresta C, in the
325 hinterland of Pernambuco, Brazil.

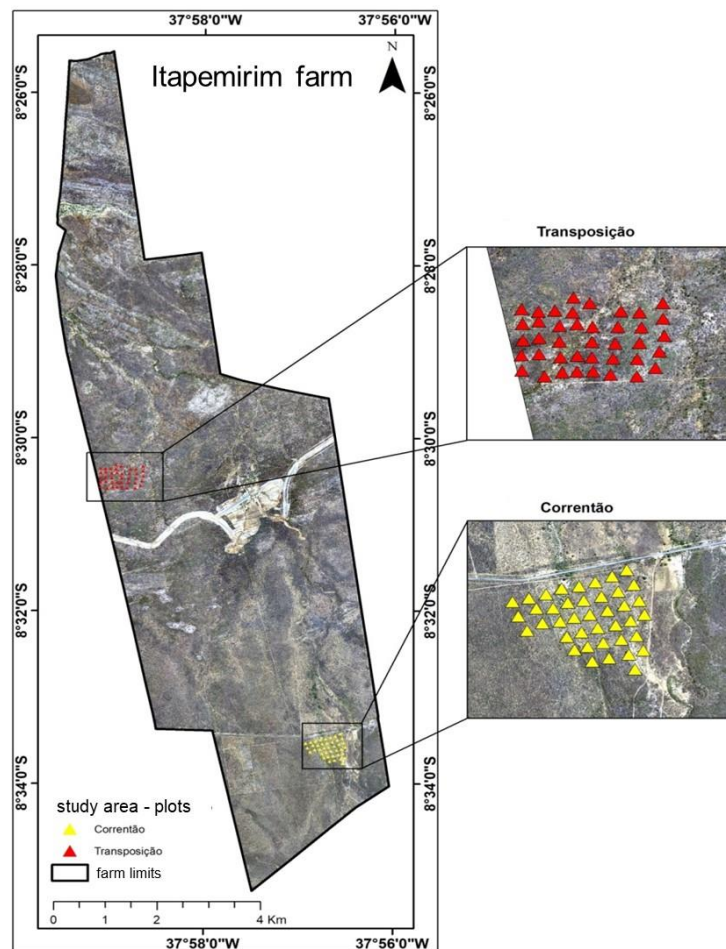
326

327 The two study areas differ from each other in terms of preservation conditions.

328 The first to the north is called “*Transposição*” with 40 permanent plots of 400 m² (20 x

329 20 m), having an extension of approximately 50 ha and is considered preserved (55
330 years of lesser anthropic disorders). The second area further south, also with 40
331 permanent plots of 400 m² (20 x 20 m) called “*Correntão*”, underwent logging using the
332 *Correntão* technique in 1987 for planting eucalyptus, but was abandoned and has been
333 undergoing regeneration for 29 years (Fig. 2).

334



335

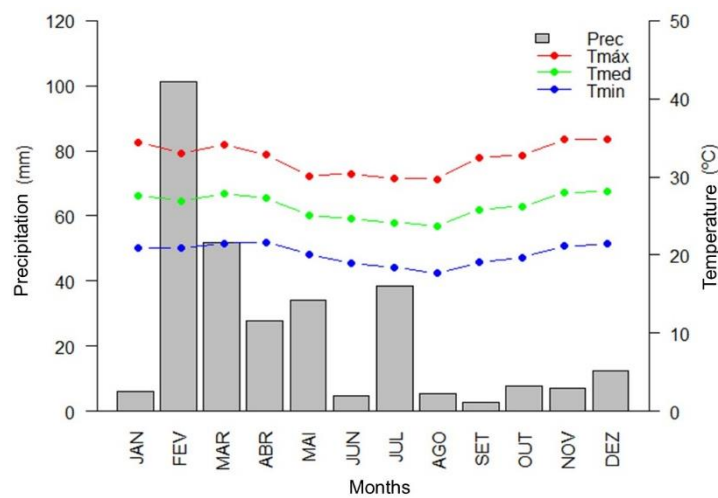
336 **Fig. 2** Sampling procedure used in the two inventoried areas in the Municipality of
337 Floresta, Pernambuco

338

339 The vegetation in these areas is predominantly Caatinga (dry tropical forest),
340 meaning savanna-steppe characterized by shrub-tree vegetation along with the presence
341 of cacti and herbaceous strata (IBGE, 2012). The climate is BSh according to the

342 Köppen classification, a hot semi-arid region with an average annual precipitation of
 343 approximately 400 to 500 mm, with a rainy period from January to April, and an
 344 average annual temperature of 26.1°C. Its distribution in temperature and precipitation
 345 throughout the year studied (2014) in the municipalities belonging to the study area are
 346 shown in Figure 3. The municipality has an area of 3,643.97 Km² and an average
 347 altitude of 323 m (EMBRAPA, 2007).

348



349

350 **Fig. 3** Distribution of air temperature and precipitation over the year 2014 in the study
 351 area by the nearest weather station. Source: Agritempo adjusted. Source: Agritempo,
 352 2018 (adjusted).

353

354 ***Estimation of the biomass/carbon stock in the field***

355 Plots, which had already been inventoried, were used to facilitate logistics and data
 356 collection in each area (Fig. 2). A total of 40 plots in each area have been monitored
 357 since 2008. They are systematically distributed and each has 20 x 20 m (400 m²). They
 358 are 80 m apart, 50 m from the edge. All arboreous individuals with circumference
 359 measured at 1.30 m above the ground (CAP) ≥ 6.0 cm were identified, labeled and
 360 measured, and the total heights (Ht) were measured by a clinometer.

361 Local biomass estimates in each plot in the different areas were generated from a
 362 previously developed local equation (Equation 1), with subsequent conversion to carbon
 363 stock ($\text{Mg}\cdot\text{ha}^{-1}$). Thus, we were able to perform local estimates of the biomass logarithm
 364 using DAP and Ht logarithms as independent variables, as shown in the equation below:
 365 $\text{TAGB} = \exp (-3.5336 + 1.9126 \times \ln (\text{DAP}) + 1.2438 \times \ln (\text{Ht}))$
 366 (1)

367 Where: DBH is the diameter of the tree at breast height (1.30 m) in cm; Ht is the height
 368 of the tree (m). This equation was developed for the site and reported an Akaike
 369 Information Criterion (AIC) value of 573.77; an adjusted determination coefficient
 370 ($R^2\text{Adj}$) of 0.90; absolute square errors (RMSE) of $18.28 \text{ kg}\cdot\text{trees}^{-1}$ and bias of 0.20
 371 $\text{kg}\cdot\text{trees}^{-1}$, respectively.

372

373 Next, the estimated biomass was converted using the average carbon fraction
 374 ($\text{CF} \approx 48\%$) of the caatinga woody species (Dalla-Lana et al. 2019) for carbon stock
 375 estimates ($\text{Mg}\cdot\text{ha}^{-1}$). In addition, it has traditionally been assumed that the carbon
 376 content of a tree's dry biomass is 50% for estimating carbon stocks for sites (Brown and
 377 Lugo, 1982; Roy et al. 2001; Malhi et al. 2004), but it should be emphasized that the
 378 carbon fraction of the wood may exhibit some small variations between species (Elias
 379 and Potvin, 2003). Thus, the carbon stock is assumed as follows:

$$380 \text{ TAGC} = \text{TAGB} \times \text{CF}$$

381 (2)

382 Where: TAGC is the estimated total aboveground carbon stock ($\text{Mg}\cdot\text{ha}^{-1}$); TAGB is the
 383 total estimated aboveground biomass ($\text{Mg}\cdot\text{ha}^{-1}$); CF is the carbon fraction (48%).

384

385 In summary, the forest inventory data analyzed for this study as well as the
 386 biomass and carbon predictions were for 2014 and are summarized in Table 1. The
 387 choice of this measurement period was defined according to the same LiDAR flyover
 388 year in the areas.

389

390 Table1. Descriptive values (mean and standard deviation) and number of individuals
 391 and total shafts sampled in the permanent plots of the study areas (2014).

Areas	DBH (cm)		Ht (m)		AGB (Mg.ha ⁻¹)		AGC (Mg.ha ⁻¹)		N° Plots	N° Ind.	N° stem
	\bar{x}	σ	\bar{x}	σ	\bar{x}	σ	\bar{x}	σ			
Transposição	3,85	2,37	3,97	0,95	9,327	5,442	4,66	27	40	1728	4576
Correntão	11,44	5,4	3,64	0,92	24,94	24,95	12,47	12,47	40	996	2903

392

393 **Estimation of the biomass/carbon stock by LiDAR data**

394 The LiDAR data used in this study were made available by the Pernambuco Three-
 395 Dimensional Program (PE3D) inserted in the Pernambuco Water Sustainability Program
 396 (PSHPE) with the objective of mapping the entire territory of the State of Pernambuco
 397 using its services covering aerophotogrammetric and laser profiling. They were
 398 collected in August 2014 using a Leica ALS50 system coupled to a BEM-810 C -
 399 Seneca II - Prefix PT-RQA aircraft, with it being possible to view their characteristics
 400 below (Table 2).

401

402 Table 2. Details of acquisition of LiDAR data.

Atributo	Valores
Lidar System	ALS-50 LEICA
Flight altitude (m)	3.068
Data de aquisição	10/08/2014
opening angle (°)	34,5
Scanner frequency (Kz; Hz)	36,8 Hz
Pulse density (pulses·m ²)	0,5
Datum	Sirgas 2000

403

404 After acquiring the point clouds of the areas to be analyzed on the Pernambuco
405 Tridimensional Program website (<http://www.pe3d.pe.gov.br/mapa.php>), it was
406 necessary to change the format from “.xyzi” to “.las ”using the LAS Utility software.
407 Thus, a descriptive report with several important characteristics of the LiDAR data set
408 was produced with the Fusion3.8 software program using the “Catalog” tool.

409 Therefore, the returns which were on the soil surface (points on the soil surface)
410 were filtered from the LiDAR point cloud using the “Ground Filter” tool. The next step
411 for both areas was to obtain the Digital Terrain Model (DTM) using the “Grid Surface
412 Create” tool and the Digital Surface Model (DSM) using the “canopy model” tool.

413 It was first necessary to normalize the data in order to carry out the subsequent
414 analyzes with the metrics of only the trees. This task was performed by subtracting the
415 DSM data from the DTM data using the “clipdata” tool. The next step was to obtain the
416 Canopy Height Digital Model (CHM) with the aid of the “canopymodel” tool to obtain
417 the metric value for each plot of the two areas, in which it was necessary to perform the
418 clipping by plot using the shape file of the plots with the point cloud using the “Polyclip
419 DATA” tool.

420 The LiDAR metrics calculate a series of estimates of descriptive statistical
421 parameters of the LiDAR point cloud and in this study were generated from the “cloud
422 metrics” tool. Thus, a total of 26 metrics were generated at the end of the data
423 processing by the point clouds in each sample unit in the different areas. These metrics
424 are the most used in biomass and carbon estimation studies, categorized according to
425 their origin and calculated symbology (Table 3).

426

427 Table 3. List of LiDAR metrics evaluated in the study, obtained from the cloudmetrics
 428 tool of the Fusion v. 3.8

Category	LiDAR metrics	Symbology
Height	Maximum height	Elev.maximum
	Minimum height	Elev.minimum
	Mean height	Elev.mean
	Modal height	Elev.mode
	Standard deviation of heights	Elev.stddev
	Height variation coefficient	Elev.CV
	Height asymmetry	Elev.skewness
	Kurtosis of height	Elev.kurtosis
	Median of absolute deviations from the general mean	Elev.MAD.median
	01th Percentile of height	Elev.P01
	05th percentile of height	Elev.P05
	10th percentile of height	Elev.P10
	20th percentile of height	Elev.P20
	25th percentile of height	Elev.P25
	30th percentile of height	Elev.P30
	40th percentile of height	Elev.P40
	50th percentile of height	Elev.P50
	60th percentile of height	Elev.P60
	70th percentile of height	Elev.P70
	75th percentile of height	Elev.P75
80th percentile of height	Elev.P80	
90th percentile of height	Elev.P90	
95th percentile of height	Elev.P95	
99th percentile of Height	Elev.P99	
Canopy density	Canopy Relief Ratio ¹	Canopy.relief.ratio
	Percentage of all returns above 1.30	Percentage.all.returns.above.1.30

429 ¹Canopyreliefratio ((HMEAN 2 HMIN)/(HMAX 2 HMIN));

430

431 Some of the main metrics used in predicting biomass and carbon are described

432 below:

433 Elev.maximum = Maximum height: this is the highest value found in the measurement

434 range in meters within each sample unit, considering variations at each meter along the

435 walking axis.

436 Elev.mean = Mean height: this is the mean value of the highest points, considering

437 variations every meter in the measurement range in meters within each sample unit

438 (Equation 3).

439 $Elev.mean = \frac{1}{n} \times \sum_{i=1}^n h_i$

440 (3)

441 Elev.stddev = Standard deviation of height in the LiDAR point cloud:

442 $Elev.stddev = \sqrt{\frac{1}{n-1} \times \sum_{i=1}^n (h_i - h_{med})^2}$

443 (4)

444 Where: hmean = mean height of the point cloud.

445 Elev.CV = Height variation coefficient in the LiDAR point cloud:

446 $h_{cv} = \frac{h_{desv}}{h_{med}}$

447 (5)

448 Height percentiles in the LiDAR point cloud (hpi): The ith percentile of n points
449 traditionally represented in the LiDAR point cloud, ordered in height values
450 corresponds to the value which occupies the K position of the data set, as in the
451 following equation:

452 $K = \frac{h_{pi}(n+1)}{100}$

453 (6)

454 Where: K = value that occupies the ith percentile in height in the point cloud; h pi = ith
455 percentile in height in the point cloud.

456

457 ***Modeling the biomass/carbon stock using LiDAR data***

458 The “R Project for Statistical Computing” Lidar Data_Analysis Tools (R Development
459 Core Team, 2017) and ArcGIS 10[®] software programs were used to construct, validate
460 and apply predictive models and generate representative biomass and forest carbon
461 maps in the different areas.

462 The LidarData_Analysis Tools software program was developed by the USDA
463 Forest Service - Remote Sensing Applications Center, written in Python language, and
464 works as an interface of R. The Lidar Data_Analysis Tools was designed to streamline
465 the statistical regression analysis process involving LiDAR metrics generated by the
466 North American Forest Service, and in fact works as a graphical interface to access the
467 statistical modeling packages available in R which simplify processing large volumes of
468 data (Silva et al., 2017a).

469 Next, three data analysis approaches were used to construct the biomass
470 allometric models per hectare according to the LiDAR metrics for the two areas:
471 Multiple linear regression, Multiple linear regression with Stepwise and Multiple linear
472 regression with Principal Components – PCA.

473 First, traditional modeling was used employing multiple linear regression. Thus,
474 it is assumed that there is a linear relationship between a Y variable (biomass; carbon)
475 and k independent variables, x_j ($j = 1, \dots, k = \text{LiDAR point cloud metrics}$). The
476 mathematical model which expresses the equation of multiple linear regression has the
477 following form:

$$478 Y = \beta_0 + \beta_1 X_1 + \beta_2 X_2 + \dots + \beta_k X_k + \varepsilon$$

479 (7)

480 Where: Y = TAGB ($\text{Mg}\cdot\text{ha}^{-1}$); β_0 = intercept on the Y axis; β_i = slope of the ith
481 explanatory variable; k = number of explanatory variables; e = random error.

482

483 Regression analysis was used with an emphasis on solving most of the forest
484 problems, especially when it is intended to obtain estimates of forest parameters through
485 biometric relationships. A careful analysis was performed in selecting the best metrics
486 from the LiDAR point cloud candidates for modeling among the metrics generated by

487 the LiDAR data processing for construction the models. According to (Silva et al.
488 2017a), Pearson's linear correlation test (r^2) should first be applied for this selection to
489 obtain the correlation between the predictive variables and to evaluate the possible
490 existence of collinearity between them. Variables with $R^2 > 0.9$ will be excluded from
491 the analysis to avoid the presence of collinearity.

492 Second, the Stepwise technique was applied using the regsubsets function of the
493 “leaps” package in R to obtain subsets of independent variables which are candidates
494 for composing the definitive biomass and carbon models in the different areas. This
495 method performs an exhaustive search to select the best combinations of independent
496 variables by minimizing Akaike’s information criterion (AIC), and rearranging them
497 into subsets which may later give rise to the selected models. Regsubsets require the use
498 of a maximum number (represented by the `nvmax` argument) of independent variables
499 for the growing construction of these subsets.

500 Third, the principal component technique (PCA) was applied to the selected
501 LiDAR metrics, and the metrics most likely to contribute to developing the model were
502 identified by inspecting the eigenvectors on each principal component. Then, the
503 metrics with the highest load on the PCs were used as input variables in multivariate
504 linear regression models that predicted biomass per hectare.

505 An example of using PCA including the equations used to obtain the
506 eigenvalues, eigenvectors and principal components (PC) can be found in Jensen
507 (2005). PCA was applied in the present study to the selected LiDAR metrics using the
508 `prcomp` function of the statistics package in R (R Core Team, 2017). A correlation
509 matrix derived from the LiDAR metrics provided the basis for calculating eigenvalues
510 and eigenvectors and for the subsequent determination of PC scores. Each score
511 represented a transformed metric from the linear combination of LiDAR metrics.

512 Differences in the contribution of each LiDAR metric to the variability in the data set,
513 as well as the similarity in the calculated metrics (Silva et al., 2017a) can be established
514 by analyzing the eigenvectors and the PC score.

515

516 ***Evaluation of models***

517 The model parameters were estimated using the Ordinary Least Squares (OLS –
518 Ordinary Least Squares) method in all the modeling methods described. The parameters
519 were generally calculated using all plots sampled in each area and will be assumed to be
520 the true parameters that represent the biomass and carbon stock at each location.

521 For each of the criteria established for the biomass estimation, the obtained
522 equations were analyzed using comparisons of statistical criteria obtained according to
523 the following equations:

$$524 R_{aj}^2 = R^2 - \left[\frac{k-1}{n-k} \right] \times (1-R^2)$$

525 (8)

$$526 RMSE = \sqrt{\frac{\sum_{i=1}^n (Y_i - \hat{Y}_i)^2}{n}}$$

527 (9)

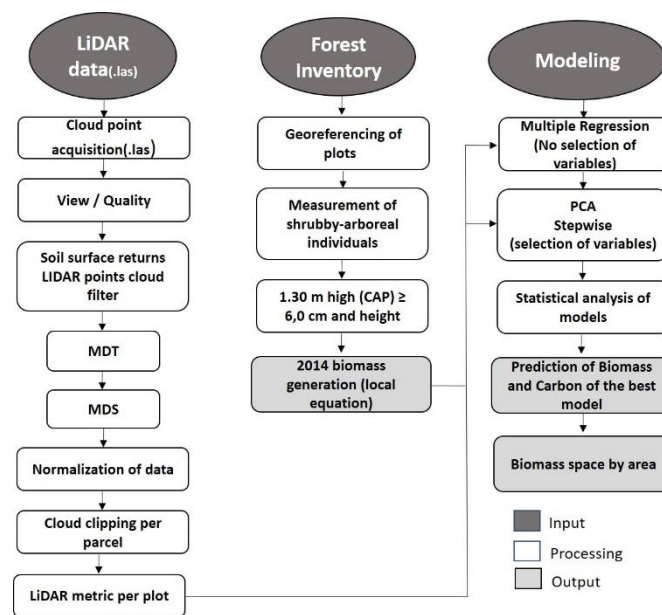
528 In which: Y_i is the replied variable (biomass and/or carbon) observed in the field (i);
529 \hat{Y}_i is the estimate (biomass and/or carbon), k is the number of parameters and n is the
530 total number of observations.

531

532 ***Generation of stock maps using LiDAR data***

533 After selecting the best model, the AsciiGrid Input function, available in the yaInpute in
534 R package (Crookston and Finley, 2007), was used to view the estimates generated by
535 the model on a map. The map expresses a grid where each cell represents a 5x5 m grid

536 colored according to the biomass and the estimated carbon content for that cell. The
 537 adopted methodology can be seen in the organization chart below (Fig. 4).



539 **Fig. 4** Flowchart of the methodology adopted and the resulting products.

540 **List of abbreviations**

541 IBGE – Instituto Brasileiro de Geografia e Estatística

542 EMBRAPA – Empresa Brasileira de Pesquisa Agropecuária

543 TAGB – Total aboveground biomass

544 TAGC – Total aboveground carbon

545

546 **Availability of data and materials**

547 The data are available upon a reasonable request to the Authors.

548 **Ethics approval and consent to participate**

549 Not applicable.

550 **Consent for publication**

551 Not applicable.

552 **Competing interests**

553 The authors declare no conflict of interest

554 **Funding**

555 Not applicable.

556

557 **Authors' contributions**

558 Cinthia Oliveira and Rinaldo Ferreira planned the study and wrote the manuscript,
559 Cinthia Oliveira, Robson Lima and José Aleixo da Silva participated in the processing
560 data LiDAR, calculation and modeling of the data and wrote the manuscript. Emanuel
561 Silva, Josias Divino Lucena, Anderson da Silva, Nattan Adler dos Santos, Cybelle
562 Souto Maior, Mayara Pessoa, Iran Jorge collected and processed the data inventory.
563 They also commented on the manuscript. The authors read and approved the final
564 manuscript.

565

566 **Acknowledgements**

567 The authors are grateful for the help of the researchers Rinaldo Caraciolo Ferreira, José
568 Aleixo da Silva and Robson Lima who collaborated to complete this work. We also
569 thank the forestry worker and German Cespedez, who is responsible for the data access
570 to the area for developing this work. The authors are grateful for the financial support
571 granted by the National Council for Scientific and Technological Development (CNPq)
572 by the productivity bag of the second and third co-authors, project leaders.

573

574 **Authors' Information**

575 Cinthia Pereira de Oliveira - <https://orcid.org/0000-0001-5158-7866>

576 Rinaldo Luiz Caraciolo Ferreira - <https://orcid.org/0000-0001-7349-6041>

577 José Antônio Aleixo da Silva - <https://orcid.org/0000-0003-0675-3524>

578 Robson Borges de Lima - <https://orcid.org/0000-0001-5915-4045>

580 **References**

- 581 Achard F, House JI. 2015. Reporting carbon losses from tropical deforestation with
582 Pan-tropical biomass maps. *Environ Res Lett.* 10(10):101002.
- 583 Althoff TD, Menezes RSC, Pinto A de S, Pareyn FGC, Carvalho AL de, Martins JCR,
584 de Carvalho EX, Silva ASA da, Dutra ED, Sampaio EV de SB. 2018. Adaptation of the
585 century model to simulate C and N dynamics of Caatinga dry forest before and after
586 deforestation. *Agric Ecosyst Environ.* 254:26–34.
- 587 Anderson KE, Glenn NF, Spaete LP, Shinneman DJ, Pilliod DS, Arkle RS, McIlroy SK,
588 Derryberry DR. 2018. Estimating vegetation biomass and cover across large plots in
589 shrub and grass dominated drylands using terrestrial lidar and machine learning. *Ecol*
590 *Indic.* 84:793–802.
- 591 Avitabile V, Herold M, Henry M, Schmillius C. 2011. Mapping biomass with remote
592 sensing: a comparison of methods for the case study of Uganda. *Carbon Balance Manag*
593 [Internet]. [accessed 2018 Sep 27] 6(1).
594 <https://cbmjournals.biomedcentral.com/articles/10.1186/1750-0680-6-7>
- 595 Becknell JM, Keller M, Piotta D, Longo M, Nara dos-Santos M, Scaranello MA, Bruno
596 de Oliveira Cavalcante R, Porder S. 2018. Landscape-scale lidar analysis of
597 aboveground biomass distribution in secondary Brazilian Atlantic Forest. *Biotropica.*
598 50(3):520–530.
- 599 Brahma B, Nath AJ, Sileshi GW, Das AK. 2018. Estimating biomass stocks and
600 potential loss of biomass carbon through clear-felling of rubber plantations. *Biomass*
601 *Bioenergy.* 115:88–96.
- 602 Brown S, Lugo AE. 1982. The storage and production of organicmatter in tropical
603 forests and their role in the global carboncycle. *Biotropica.* 14:161–187
- 604 Chave J, Andalo C, Brown S, Cairns MA, Chambers JQ, Eamus D, Fölster H, Fromard
605 F, Higuchi N, Kira T, et al. 2005. Tree allometry and improved estimation of carbon
606 stocks and balance in tropical forests. *Oecologia.* 145(1):87–99.
- 607 Chave J, Réjou-Méchain M, Búrquez A, Chidumayo E, Colgan MS, Delitti WBC,
608 Duque A, Eid T, Fearnside PM, Goodman RC, et al. 2014. Improved allometric models
609 to estimate the aboveground biomass of tropical trees. *Glob Change Biol.* 20(10):3177–
610 3190.
- 611 Chen Q, Lu D, Keller M, dos-Santos M, Bolfe E, Feng Y, Wang C. 2015. Modeling and
612 Mapping Agroforestry Aboveground Biomass in the Brazilian Amazon Using Airborne
613 Lidar Data. *Remote Sens.* 8(1):21.
- 614 Coomes DA, Dalponte M, Jucker T, Asner GP, Banin LF, Burslem DFRP, Lewis SL,
615 Nilus R, Phillips OL, Phua M-H, Qie L. 2017. Area-based vs tree-centric approaches to
616 mapping forest carbon in Southeast Asian forests from airborne laser scanning data.

- 617 Remote Sens Environ [Internet]. [accessed 2018 Nov 12] 194:77–88.
618 <https://linkinghub.elsevier.com/retrieve/pii/S0034425717301098>
- 619 Crookston NL, Finley A. 2008. Yaimpute: An R package for k-NN imputation. *Journal*
620 *of Statistical Software*. 23(10): 1–16. <https://doi.org/10.18637/jss.v023.i10>.
- 621 Crowther TW, Glick HB, Covey KR, Bettigole C, Maynard DS, Thomas SM, Smith JR,
622 Hintler G, Duguid MC, Amatulli G, et al. 2015. Mapping tree density at a global scale.
623 *Nature*. 525(7568):201–205.
- 624 Dalla Lana M. et al. 2018. Biomass equations for caatinga species. *Nativa* 6:517–525.
625 <http://dx.doi.org/10.31413/nativa.v6i5.5361>
- 626 Duncanson L, Huang W, Johnson K, Swatantran A, McRoberts RE, Dubayah R. 2017.
627 Implications of allometric model selection for county-level biomass mapping. *Carbon*
628 *Balance Manag* [Internet]. [accessed 2018 Aug 16] 12(1).
629 <https://cbmjournl.biomedcentral.com/articles/10.1186/s13021-017-0086-9>
- 630 Elias M, Potvin C. 2003. Assessing inter- and intra-specific variation in trunk carbon
631 concentration for 32 neotropical tree species. **Canadian Journal of Forest Research**.
632 33(6): 1039–1045. <https://doi.org/10.1139/x03-018>.
- 633 Empresa Brasileira de Pesquisa Agropecuária- EMBRAPA. Zoneamento Agroecológico
634 do Estado de Pernambuco – ZAPE. 2007. Disponível em:
635 <http://www.uep.cnps.embrapa.br/zape>. Acesso em: 15 abr. 2017.
- 636 Figueiredo EO, d'Oliveira MVN, Braz EM, de Almeida Papa D, Fearnside PM. 2016.
637 LIDAR-based estimation of bole biomass for precision management of an Amazonian
638 forest: Comparisons of ground-based and remotely sensed estimates. *Remote Sens*
639 *Environ* [Internet]. [accessed 2018 Nov 12] 187:281–293.
640 <https://linkinghub.elsevier.com/retrieve/pii/S0034425716303984>
- 641 Hernández-Stefanoni JL, Johnson KD, Cook BD, Dupuy JM, Birdsey R, Peduzzi A,
642 Tun-Dzul F. 2015. Estimating species richness and biomass of tropical dry forests using
643 LIDAR during leaf-on and leaf-off canopy conditions. Goslee S, editor. *Appl Veg Sci*.
644 18(4):724–732.
- 645 Instituto Brasileiro de Geografia e Estatística, Coordenação de Recursos Naturais e
646 Estudos Ambientais. 2012. Manual técnico da vegetação brasileira.
- 647 Jensen JR. 2005. *Introductory digital image processing: a remote sensing perspective*.
648 Upper Saddle River, N.J: Prentice Hall.
- 649 Kachamba D, Ørka H, Næsset E, Eid T, Gobakken T. 2017. Influence of Plot Size on
650 Efficiency of Biomass Estimates in Inventories of Dry Tropical Forests Assisted by
651 Photogrammetric Data from an Unmanned Aircraft System. *Remote Sens*. 9(6):610.
- 652 Leitold V, Keller M, Morton DC, Cook BD, Shimabukuro YE. 2015. Airborne lidar-
653 based estimates of tropical forest structure in complex terrain: opportunities and trade-
654 offs for REDD+. *Carbon Balance Manag* [Internet]. [accessed 2018 Nov 12] 10(1).
655 <https://cbmjournl.biomedcentral.com/articles/10.1186/s13021-015-0013-x>

656 Li A, Dhakal S, Glenn N, Spaete L, Shinneman D, Pilliod D, Arkle R, McIlroy S. 2017.
657 Lidar Aboveground Vegetation Biomass Estimates in Shrublands: Prediction,
658 Uncertainties and Application to Coarser Scales. *Remote Sens.* 9(9):903

659 Magnusson M. et al. 2007. Effects on Estimation Accuracy of Forest Variables Using
660 Different Pulse Density of Laser Data. *Forest Science.* 53(6): 619-626. Disponível em:
661 <https://pub.epsilon.slu.se/3651/>. Acesso em: 22 jun. 2018.

662 Malhi, Y. et al. 2004. The above-ground coarse wood productivity of 104 Neotropical
663 forest plots. *Global Change Biology.* 10(5): 563–591. [https://doi.org/10.1111/j.1529-](https://doi.org/10.1111/j.1529-8817.2003.00778.x)
664 [8817.2003.00778.x](https://doi.org/10.1111/j.1529-8817.2003.00778.x).

665 Martinuzzi S, Gould WA, Vierling LA, Hudak AT, Nelson RF, Evans JS. 2013.
666 Quantifying Tropical Dry Forest Type and Succession: Substantial Improvement with
667 LiDAR. *Biotropica.* 45(2):135–146.

668 Mohebalian PM, Aguilar FX. 2018. Beneath the Canopy: Tropical Forests Enrolled in
669 Conservation Payments Reveal Evidence of Less Degradation. *Ecol Econ.* 143:64–73.

670 Naveenkumar J, Arunkumar KS, Sundarapandian Sm. 2017. Biomass and carbon stocks
671 of a tropical dry forest of the Javadi Hills, Eastern Ghats, India. *Carbon Manag.* 8(5–
672 6):351–361.

673 Nelson R, Margolis H, Montesano P, Sun G, Cook B, Corp L, Andersen H-E, deJong B,
674 Pellat FP, Fickel T, et al. 2017. Lidar-based estimates of aboveground biomass in the
675 continental US and Mexico using ground, airborne, and satellite observations. *Remote*
676 *Sens Environ* [Internet]. [accessed 2018 Nov 12] 188:127–140.
677 <https://linkinghub.elsevier.com/retrieve/pii/S0034425716304175>

678 R Core Team. 2017. R: A language and environment for statistical computing. R
679 Foundation for Statistical Computing, Vienna, Austria. URL [https://www.R-](https://www.R-project.org/)
680 [project.org/](https://www.R-project.org/).

681 Roy J. 2001. *Terrestrial global productivity*. San Diego: Academic.

682 Saatchi S, Malhi Y, Zutta B, Buermann W, Anderson LO, Araujo AM, Phillips OL,
683 Peacock J, ter Steege H, Lopez Gonzalez G, et al. 2009. Mapping landscape scale
684 variations of forest structure, biomass, and productivity in Amazonia. *Biogeosciences*
685 *Discuss.* 6(3):5461–5505.

686 Sampaio EV, Silva GC. 2005. Biomass equations for Brazilian semiarid caatinga plants.
687 *Acta Bot Bras.* 19(4):935–943.

688 Silva C, Hudak A, Vierling L, Klauberg C, Garcia M, Ferraz A, Keller M, Eitel J,
689 Saatchi S. 2017a. Impacts of Airborne Lidar Pulse Density on Estimating Biomass
690 Stocks and Changes in a Selectively Logged Tropical Forest. *Remote Sens.* 9(10):1068.

691 Silva C, Hudak A, Vierling L, Klauberg C, Garcia M, Ferraz A, Keller M, Eitel J,
692 Saatchi S. 2017b. Impacts of Airborne Lidar Pulse Density on Estimating Biomass
693 Stocks and Changes in a Selectively Logged Tropical Forest. *Remote Sens* [Internet].
694 [accessed 2018 Nov 12] 9(10):1068. <http://www.mdpi.com/2072-4292/9/10/1068>

- 695 Silva CA, Klauberg C, Hudak AT. 2014. Mapeamento de estoques de carbono acima do
696 solo utilizando dados LiDAR em plantações de Eucalyptus spp no estado de São Paulo,
697 Brasil. Sci For. 42(104):14.
- 698 Silva CA, Klauberg C, Hudak AT, Vierling LA, Liesenberg V, Carvalho SPC e,
699 Rodriguez LCE. 2016. A principal component approach for predicting the stem volume
700 in Eucalyptus plantations in Brazil using airborne LiDAR data. Forestry. 89(4):422–
701 433.
- 702 Somogyi Z, Cienciala E, Mäkipää R, Muukkonen P, Lehtonen A, Weiss P. 2007.
703 Indirect methods of large-scale forest biomass estimation. Eur J For Res. 126(2):197–
704 207.
- 705 Takahashi T, Awaya Y, Hirata Y, Furuya N, Sakai T, Sakai A. 2010. Stand volume
706 estimation by combining low laser-sampling density LiDAR data with QuickBird
707 panchromatic imagery in closed-canopy Japanese cedar (*Cryptomeria japonica*)
708 plantations. Int J Remote Sens [Internet]. [accessed 2018 Nov 12] 31(5):1281–1301.
709 <https://www.tandfonline.com/doi/full/10.1080/01431160903380623>
- 710 Thomas V, Treitz P, McCaughey JH, Morrison I. 2006. Mapping stand-level forest
711 biophysical variables for a mixedwood boreal forest using lidar: an examination of
712 scanning density. Can J For Res [Internet]. [accessed 2018 Nov 12] 36(1):34–47.
713 <http://www.nrcresearchpress.com/doi/10.1139/x05-230>

Figures

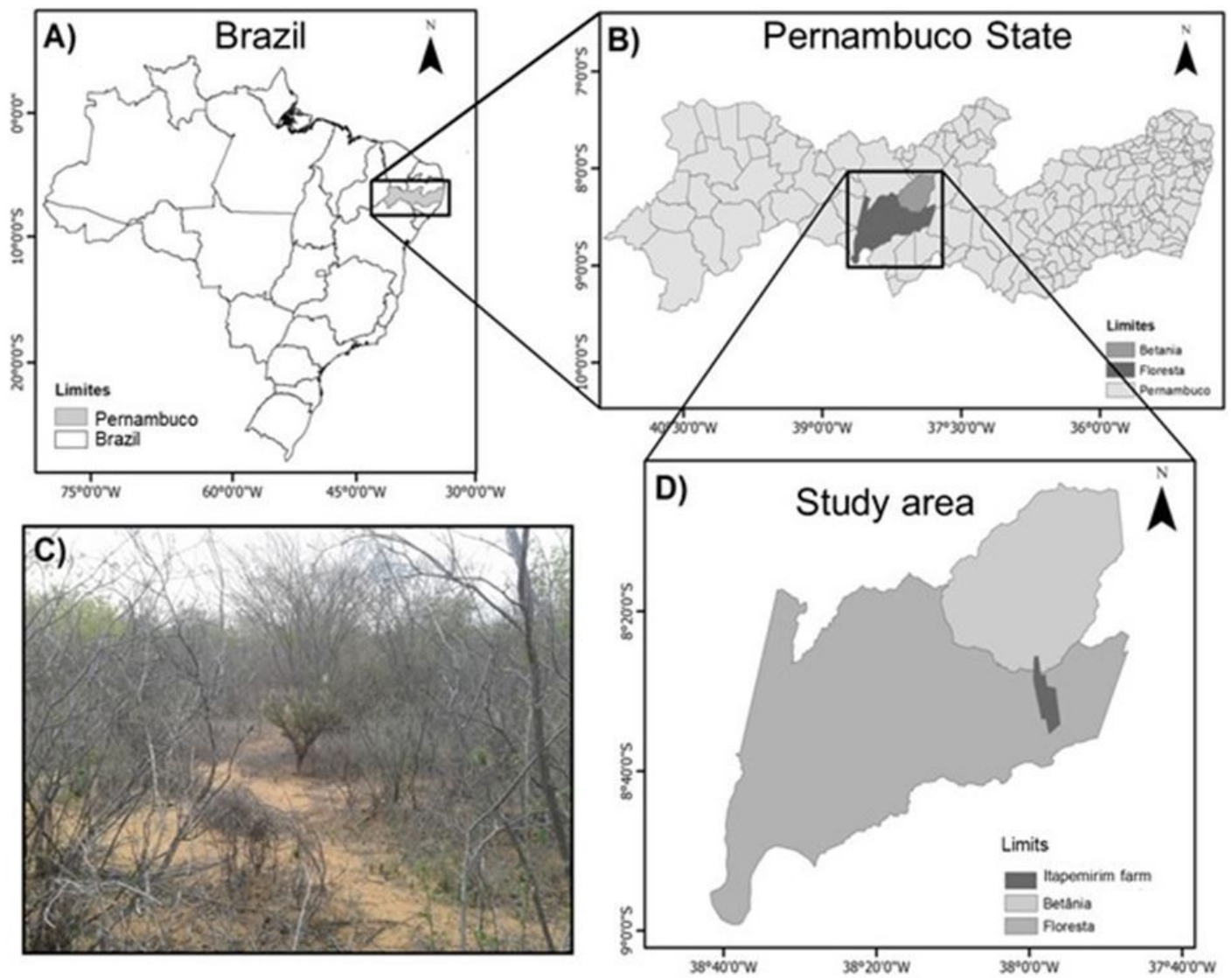


Figure 1

Coverage of the study area: A, B and D, and profile photo in Floresta C, in the hinterland of Pernambuco, Brazil.

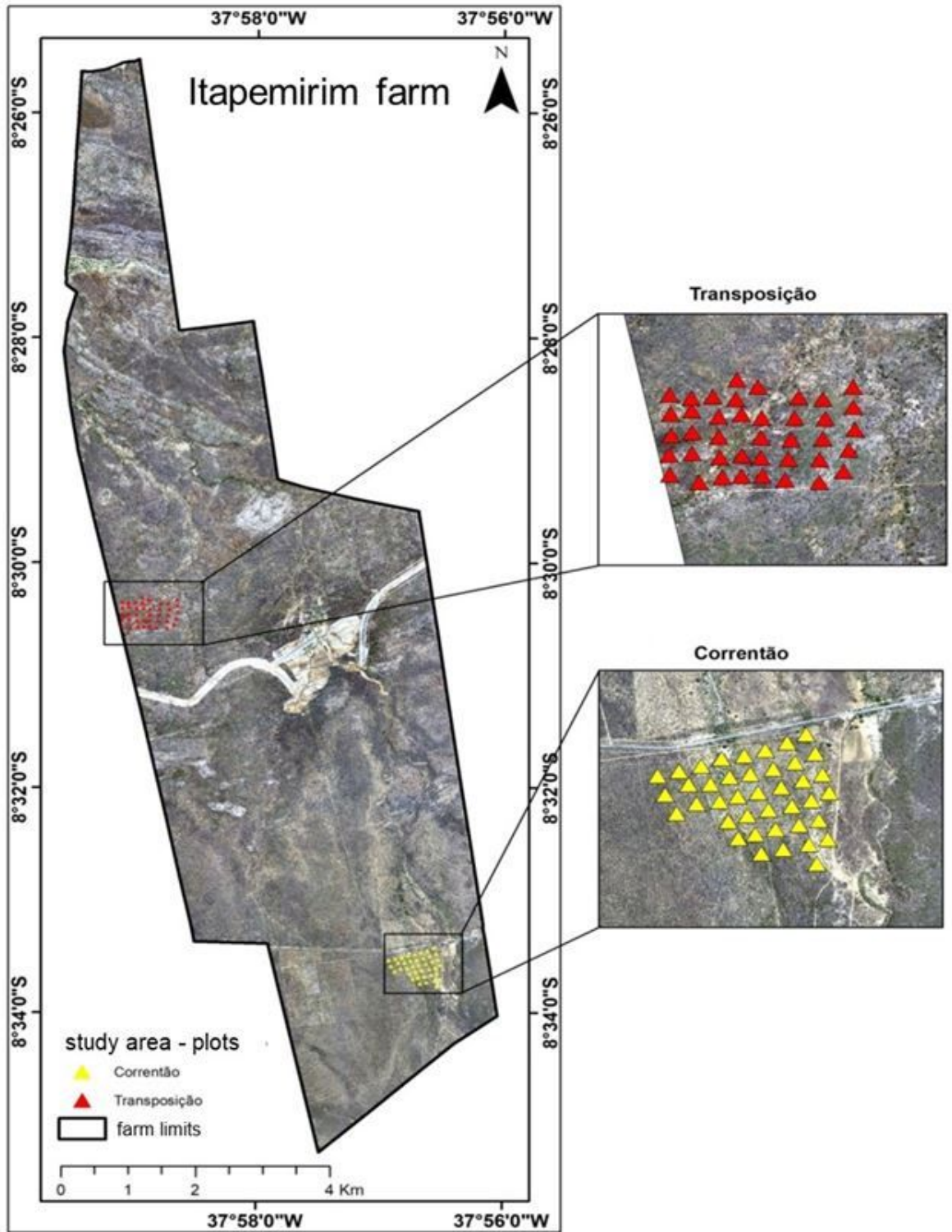


Figure 2

Sampling procedure used in the two inventoried areas in the Municipality of Floresta, Pernambuco.

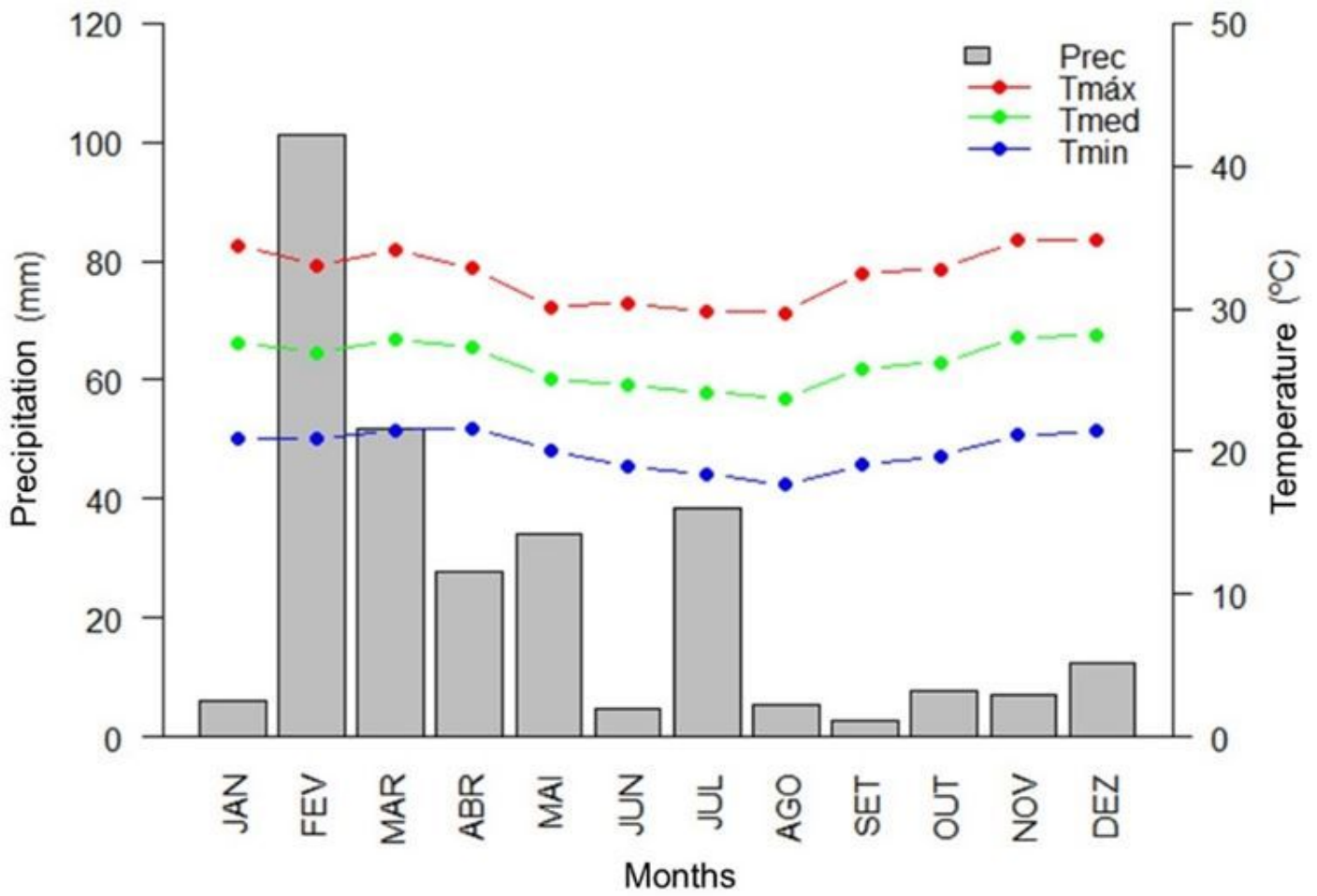


Figure 3

Distribution of air temperature and precipitation over the year 2014 in the study area by the nearest weather station. Source: Agritempo adjusted. Source: Agritempo, 2018 (adjusted).

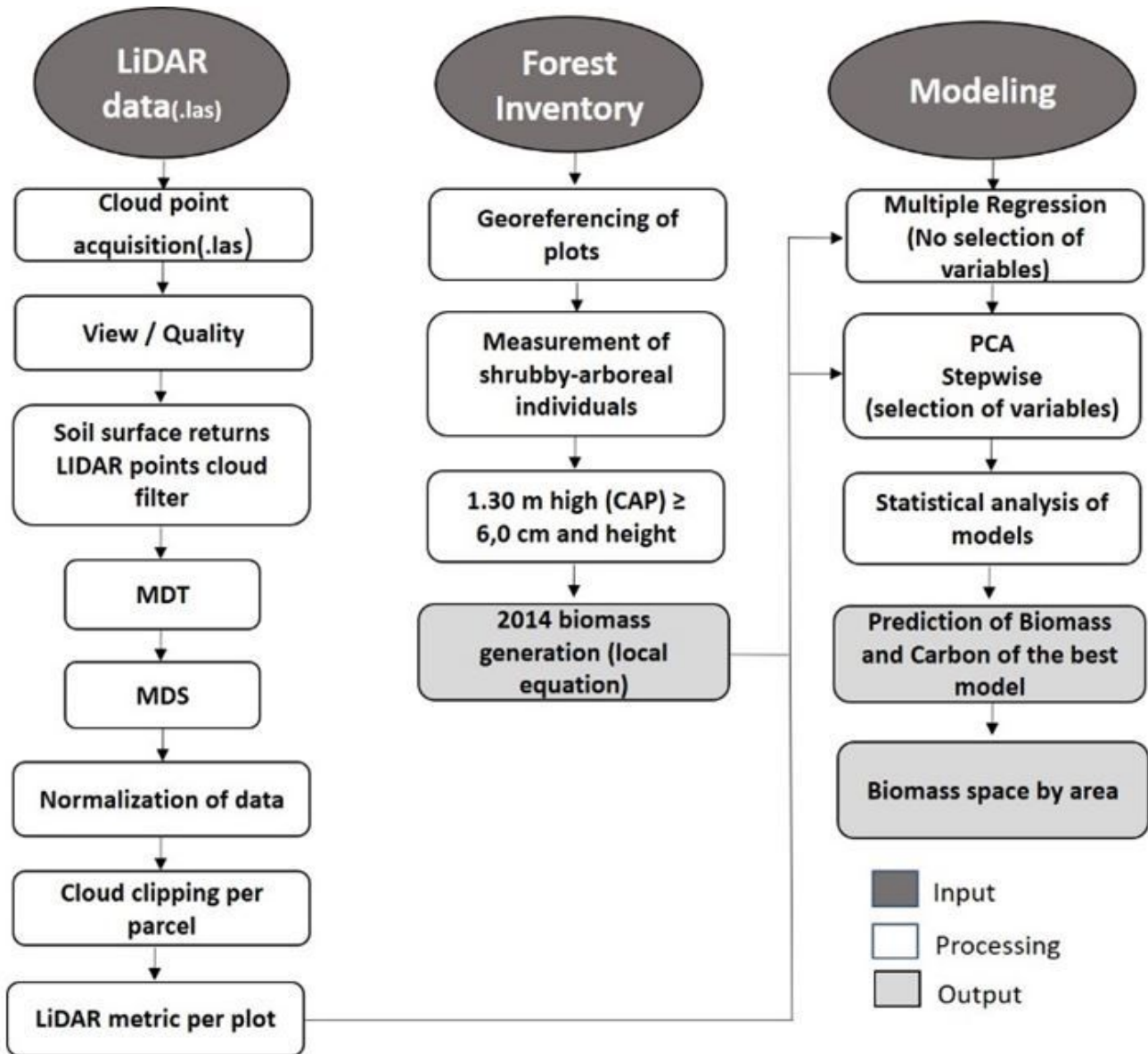


Figure 4

Flowchart of the methodology adopted and the resulting products.

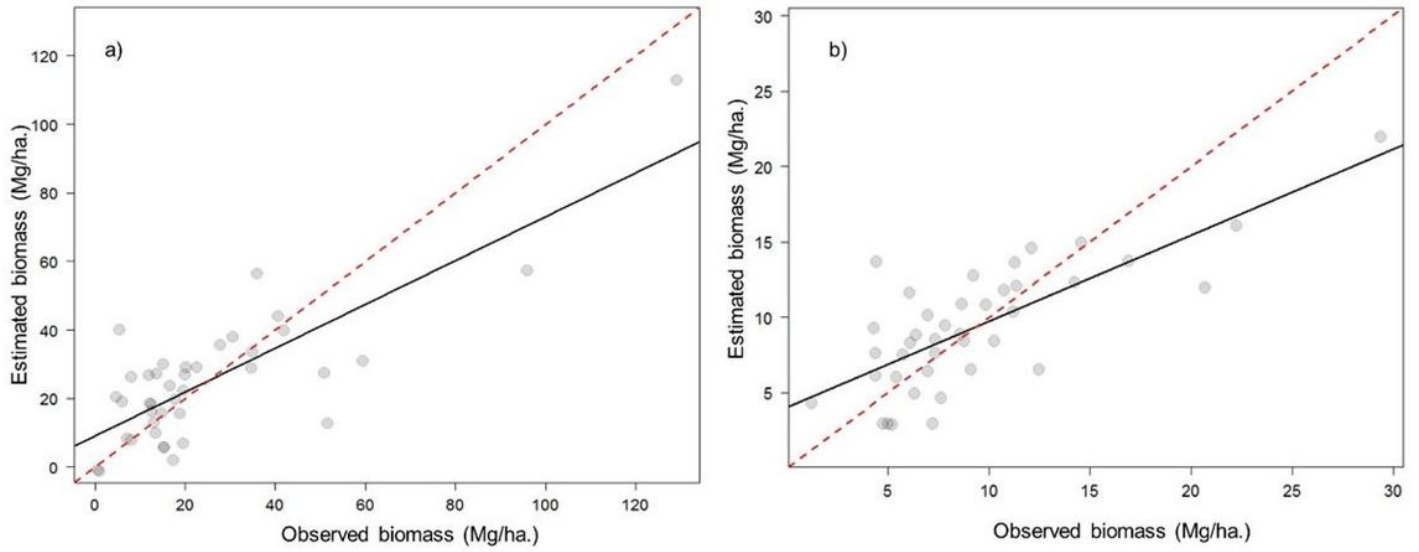


Figure 5

Predictions of the best allometric equations for the Correntão area (a) and Transposição (b) using the LiDAR metrics selected step by step in relation to the observed values. The solid black line indicates the fit of the equation and the red dotted line indicates the ideal fit in a 1: 1 ratio.

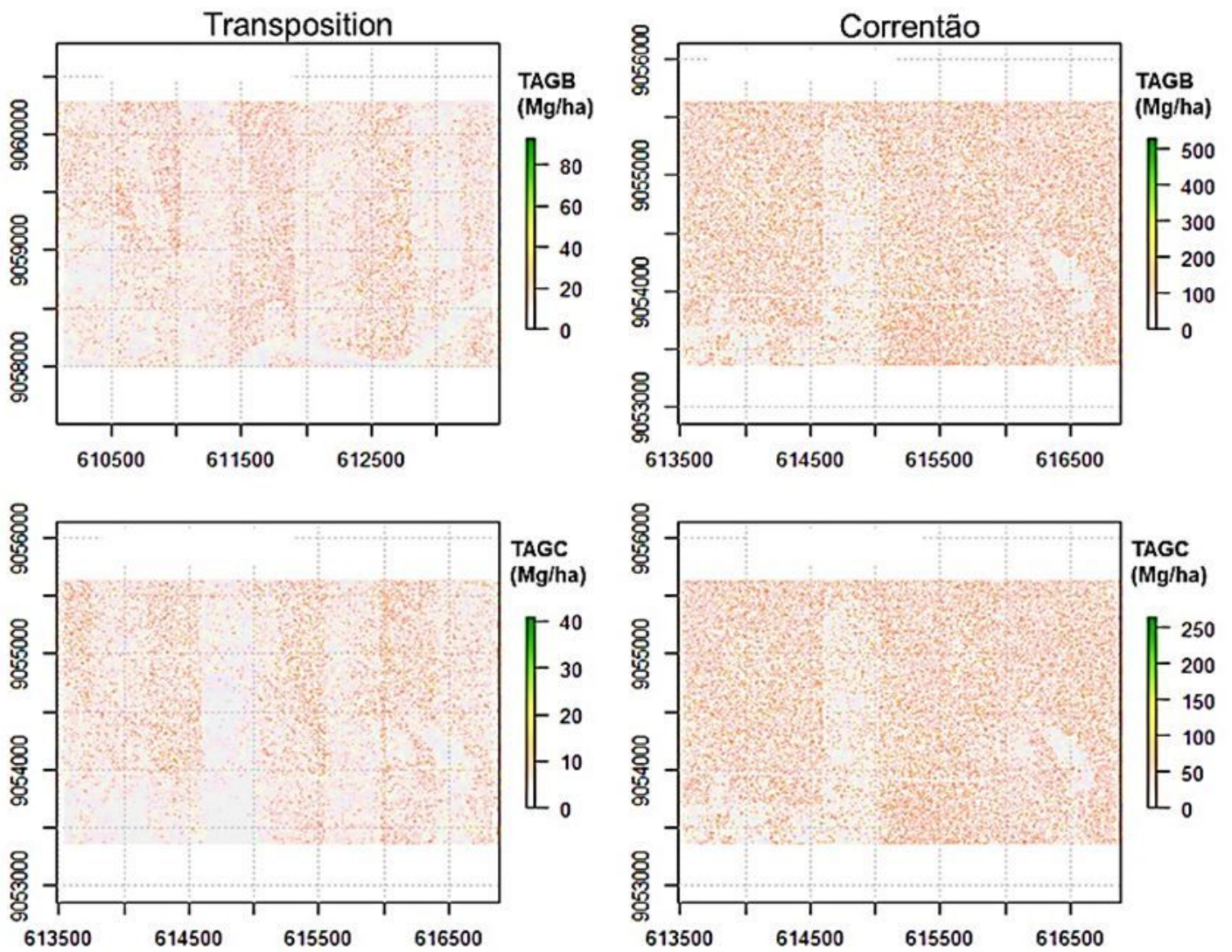


Figure 6

Spatialization of biomass and carbon based on Stepwise regression models defined according to the LiDAR metrics for the Transposição and Correntão areas.